ISSN: 0067-2904

Electrochemical Polymerization and Biological Activity of 4-(Nicotinamido)-4-Oxo-2-Butenoic Acid as An Anticorrosion Coating on A 316L Stainless Steel Surface

Khulood A. Saleh*, Sana A. Habeeb
Department of Chemistry, College of Science, University of Baghdad, Baghdad, Iraq

Received: 18/4/2020 Accepted: 9/8/2020

Abstract

In this study, poly4-(nicotinamido)-4-oxo-2-butenoic acid (PNOE) was prepared by the electro polymerization of 4-(nicotinamido)-4-oxo-2-butenoic acid (NOE) monomer on a 316 stainless steel (St.St) which acts as an anticorrosion coating. Fourier transforms infrared (FTIR), atomic force microscopy (AFM), scanning electron microscopy (SEM), and cyclic voltammetry were used to diagnose the structure and the properties of the prepared polymer layer. The corrosion behavior of the uncoated and coated 316 St.St were evaluated by using an electro chemical polarization technique in 0.2 M hydrochloric acid solution as a corrosive medium at a temperature range of 293 to 323 K. Nano materials, such as nano ZnO and graphene were added in different concentrations to the monomer solution for improving the corrosion resistance of the 316 St.St surface. The results showed that the values of protection efficiencies of the polymeric coating were increased after adding the nano materials. The kinetic and thermodynamic activation parameters were also calculated and the biological activity of the polymer film against Gram negative and positive bacteria was studied.

Keywords: corrosion, electro chemical polymerization, stainless steel, coating, nicotinamide, nanomaterial, Antibacterial activity.

البلمرة الكهربائية (لنيكوتين اميدو)- اوكسو- حامض البيوتينوك على سطح الفولاذ الصلب 316 كطلاء مضاد للتآكل ودراسة الفعالية البايولوجية له

خلود عبد صالح ، سناء حبيب

قسم الكيمياء، كلية العلوم، جامعة بغداد، بغداد، العراق

الخلاصه

في هذه الدراسة تم تحضير البولي (نيكوتين اميدو)- اوكسو- حامض البيوتينوك بواسطة البلمرة الكهروكيميائية لمونومر (نيكوتين اميدو)- اوكسو – حامض البيوتينوك كطلاء مضاد للتآكل . تم أستخدام تقنية الاشعة تحت الحمراء , مجهرالمسح الالكتروني, مجهرالقوة الذرية والجهد الدوري لتشخيص بنية وخصائص طبقة البوليمر المحضرة. تم تقدير سلوك التآكل للفولاذ الصلب المطلي وغيرالمطلي باستخدام تقنية الاستقطاب الكهروكيميائي في محلول 0.2 مولاري حامض الهيدروكلوريك المخفف كوسط تآكل عند درجات حرارية من 293 الى323 كلفن تم اضافة المواد النانوية (اوكسيد الزنك النانوي و الكرافين) الى محلول المونومر لتحسين مقاومة سطح الفولاذ الصلب ضد التآكل , أظهرت النتائج أن قيم كفاءة الحماية للطلاء

*Email: salkhfaji110@gmail.com

البوليمري تزداد بعد أضافة المواد النانوية. كذلك تم حساب الدوال الحركية والثرموديناميكية لعملية التآكل, أيضا تمت دراسة الفعالية البايولوجية لفلم البوليمر ضد البكتيريا السالبة والبكتيريا الموجبة.

1-Introduction

Despite much progress in the sciences and technologies of corrosion protection and control, the phenomenon of corrosion, usually of metals and alloys, continues to pose a major apprehension to many industries around the world. Generally, corrosion can be prevented by proper modifications in the environment (addition of inhibitors), material (selection of corrosion resistant materials), and material surfaces (coatings and films). Due to its properties, St.St is a common construction material with applications in various industries and an excellent choice when good corrosion resistance is required. The corrosion resistance of St.St is associated with the formation of a thin passive film on the alloy surface [1] . The stability of the natural thin layer may be violated in aggressive chloride environments, which can result in the development of localized pitting corrosion and irreversible damage to the steel products [2]. Corrosion resistance of St.St in the presence of chloride ions can be developed by the application of a protective coating, which has been widely used for the control of metal corrosion [3]. The use of conducting polymers for the protection against corrosion is an area which is recently gaining an increasing attention [4].

Conducting polymers can be prepared from aqueous or organic solvents by chemical or electrochemical polymerization [5]. The electrochemical technique is generally preferred since it supplies better control of film thickness and morphology via different parameters, such as current density, pH , monomer concentration, and nature of electrolyte solution [6-8]. Different electro-polymerization techniques can be used, including galvanostatic (constant current), potentiostatic (constant potential), and potentiodynamic (cyclic voltammetry) techniques. Conducting polymers are electrically conductive because of their extensive π- conjugated backbone. The degree of conductivity is affected by the density and mobility of electrons [9]. The conductive properties render polymer coating materials ideal candidates for metal protection [10]. They also have other applications, such as there usage in sensors [11] , energy storage systems [12] , batteries [13] , molecular devices [14], membrane gas separation [15] , and solar cells [16]. The use of coatings which have antibacterial activity is an efficient method to decrease microbial numbers on the healthcare facilities. Antibacterial agents are materials that can kill pathogenic microorganisms [17]. Good antimicrobial polymers must be biocidal to broad spectra of pathogenic microorganisms, insoluble in water for variable applications, and unlikely to decompose to toxic materials [18, 19] .

In this work, the polymeric film (PONE) was prepared by the electro-polymerization of the monomer (NOE) on St.St surface. The characterization of PONE was achieved by using SEM, AFM, FTIR, and the cyclic voltammetry method. The corrosion protection tests of uncoated and coated St.St in 0.2M HCl solution at temperatures of 293 to 323 K were conducted by using the electrochemical polarization technique. The effects of adding the nanomaterials (nano ZnO and Graphene) were studied to develop the anti-corrosion coating by polymerization.

2- Experimental Part

2.1. Synthesis of the NOE Monomer

4-(nicotinamido)-4-oxo-2-butenoic acid was synthesized by the following procedure. Maleic anhydride (1g, 0.01mol) was dissolved in 20ml of dioxane. Nicotineamide (1g, 0.01mol) was added to the reaction mixture and stirred for 6h at room temperature. The dark yellow precipitate was formed, filtered, and dried under vacuum. Figure-1 illustrates the formula applied for the synthesis of NOE.

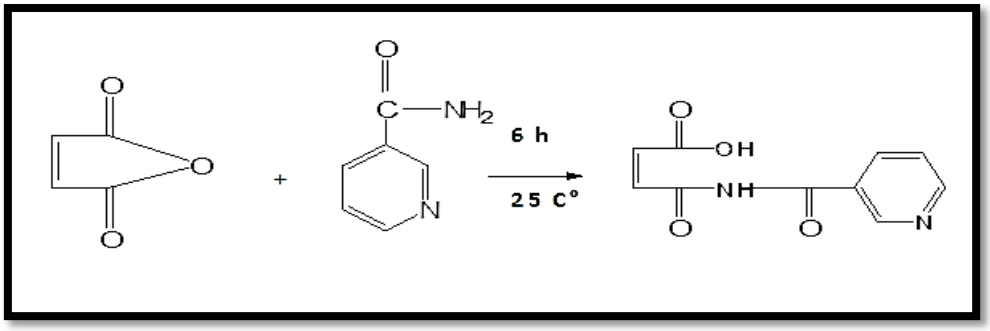

Figure 1- The chemical formula applied for the synthesis of NOE.

2.2. Electro-polymerization of NOE

The electro-polymerization of NOEon the 316 St.St surface (anodic electrode) was performed by using regular DC power supply (Galvanostatic technique). The electrodes were cleaned, washed by distilled water and acetone, and then dried. The solution which was utilized for the polymerization process was prepared by dissolving 0.1g of NOE in 100 ml of H_2O, with three drops of H_2SO_4 (95%) as a supporting electrolyte [20]. The polymeric film was deposited on the anodic electrode at room temperature. Graphene (0.004g) was added to the monomer solution after dispersing it, followed by the addition of 0.04g of nano-ZnO to develop the polymeric coating against corrosion and microbial activities.

2.3 Electrochemical Corrosion measurement

For corrosion measurement, three types of electrodes were utilized, including reference electrode (SCE), working electrode (St.St, coated or uncoated), and auxiliary electrode (platinum electrode). Anodic and cathodic polarizations for the corrosion of coated and uncoated St.St were performed under potentiostatic conditions in 0.2M HCl at a temperature range of 293 to 323 K.

2.4 Electro-deposition of PNOE on St.St by cyclic voltammetry

The electro-deposition of PNOE film on St.St electrode was conducted through the electro polymerization of the aqueous solution containing 0.2g NOE, 200ml H_2O, and 3 drops of H_2SO_4 (95%) by cyclic voltammetry during a potential range of -2000 to 2000mV and a scan rate of 40mV/s.

3- Results and discussion

3.1 The electrochemical cyclic voltammetry of PNOE coating

The cyclic voltammogram was utilized for the recording during the electro- deposition of PNOE film on St.St. It was used to explore the redox properties of the polymeric film. Figure-1 shows the successive cyclic voltammogram obtained with PNOE. From the first scan, it is observed that the oxidation wave starts at 1.8V, which can lead to the oxidation of the monomer. The intensity of this oxidation wave was decreased within the following scans, while the oxidation wave was shifted to the higher potential, which can be indicative to the electropolymerization of the monomer. The polymerization rate was increased when the potential was higher than 1.8V. At the end of the repetitive cycles, a green polymer coating became visible. The increases in the anodic currents were related to the electrochemical polymerization of the polymer, while these currents were decreased gradually with the increasing number of the scan. Therefore, the growth of the coating film during the cycling process resulted in the decrease in the current with increasing cycles number [21].

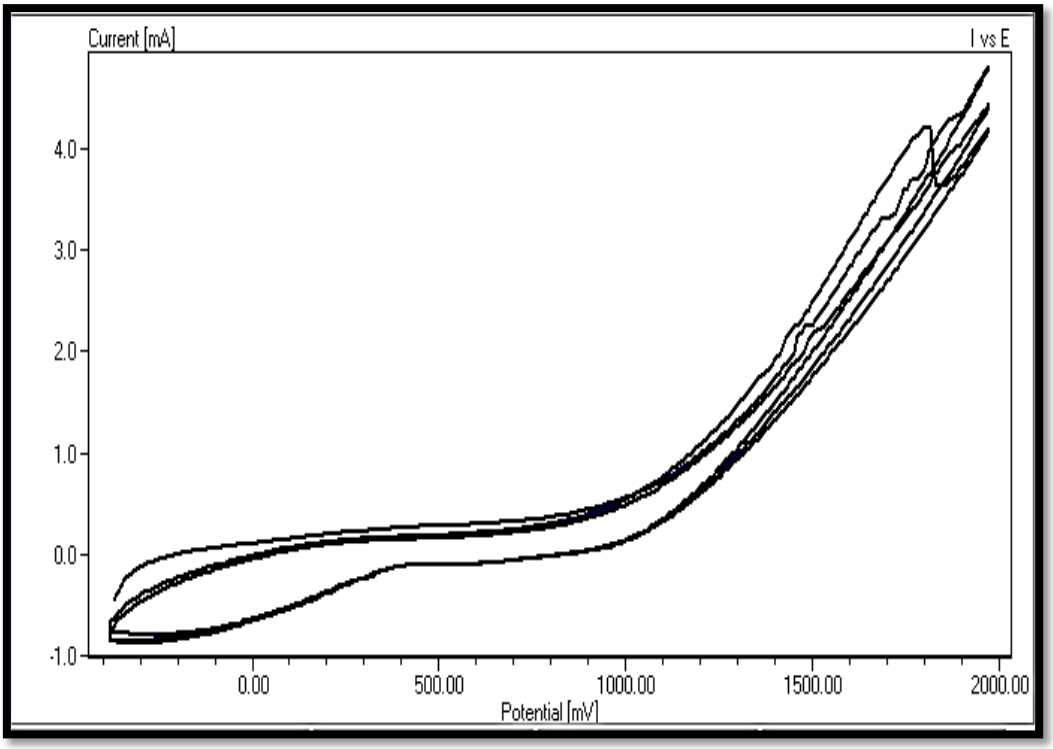

Figure 1-Cyclic voltammogram for electro-polymerization of NOE.

3.2 Mechanism of polymerization

The electro-polymerization reaction for graphting and growth of the PNOE film on the metal surface was proposed by the cationic mechanism [22, 23]. As illustrated in Scheme (1-A), the first step included the transfer of the electron from the monomer to the working electrode (metal surface) (A1). This electron transfer leads to the formation of a radical cation that adsorbs on the electrode surface, which appears in (A2). The radical cation desorbs and reacts in the solution to give rise to a component of low molecular weight (A3). Then, the NOE molecule adds through the cationic mechanism at the charged end of the adsorbed oxidized NOE (A4).

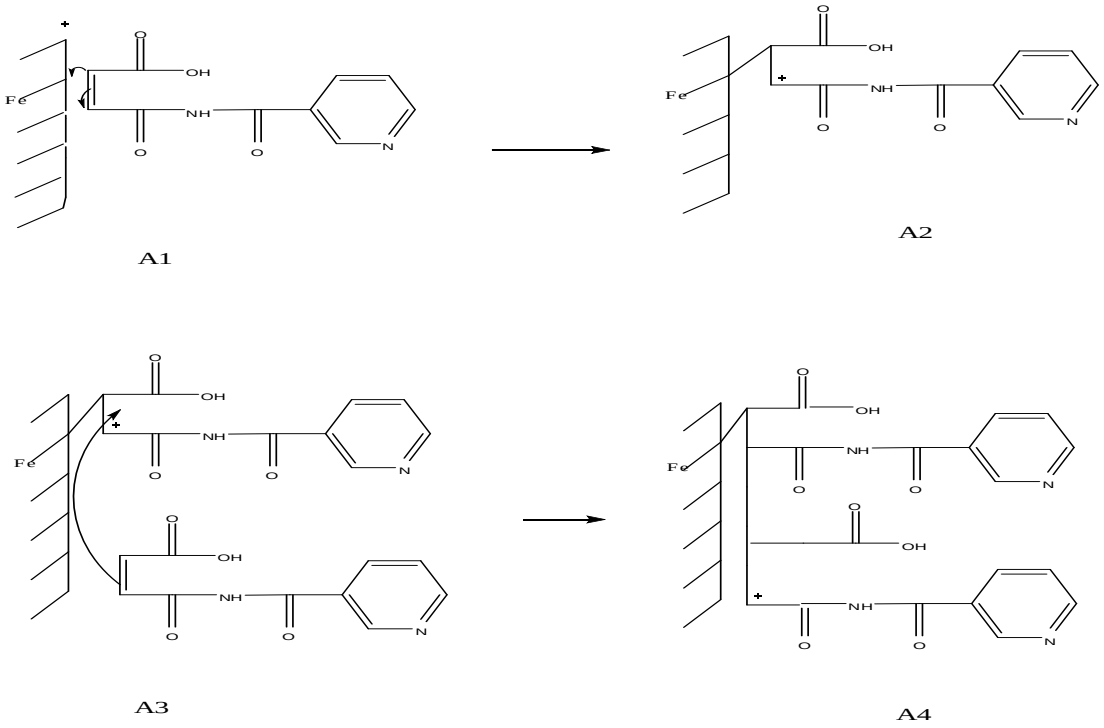

Scheme 1- Cationic mechanism for grafting and growth of PNOE films

3.3. The structure of PNOE

3.3.1 FT-IR Test

The polymer coating formed was examined by FT-IR spectroscopy. As demonstrated in Figure- 2-A, the spectrum of NOE showed the band for an aliphatic double bond (CH=CH) at 1608.52 cm^{-1}, while at the spectrum of the polymer PONE (Figure- 2-B) , this band disappeared, confirming the formation of the polymer film [24-26]. According to Figure- 1-A, the frequency peak for C=O of the carboxylic group appeared at 1704.96 cm^{-1} , the peak at 3276.83 cm^{-1} is attributed to the NH- amide group, and the absorption band of the C=O amide group appeared at 1654.81cm^{-1}.

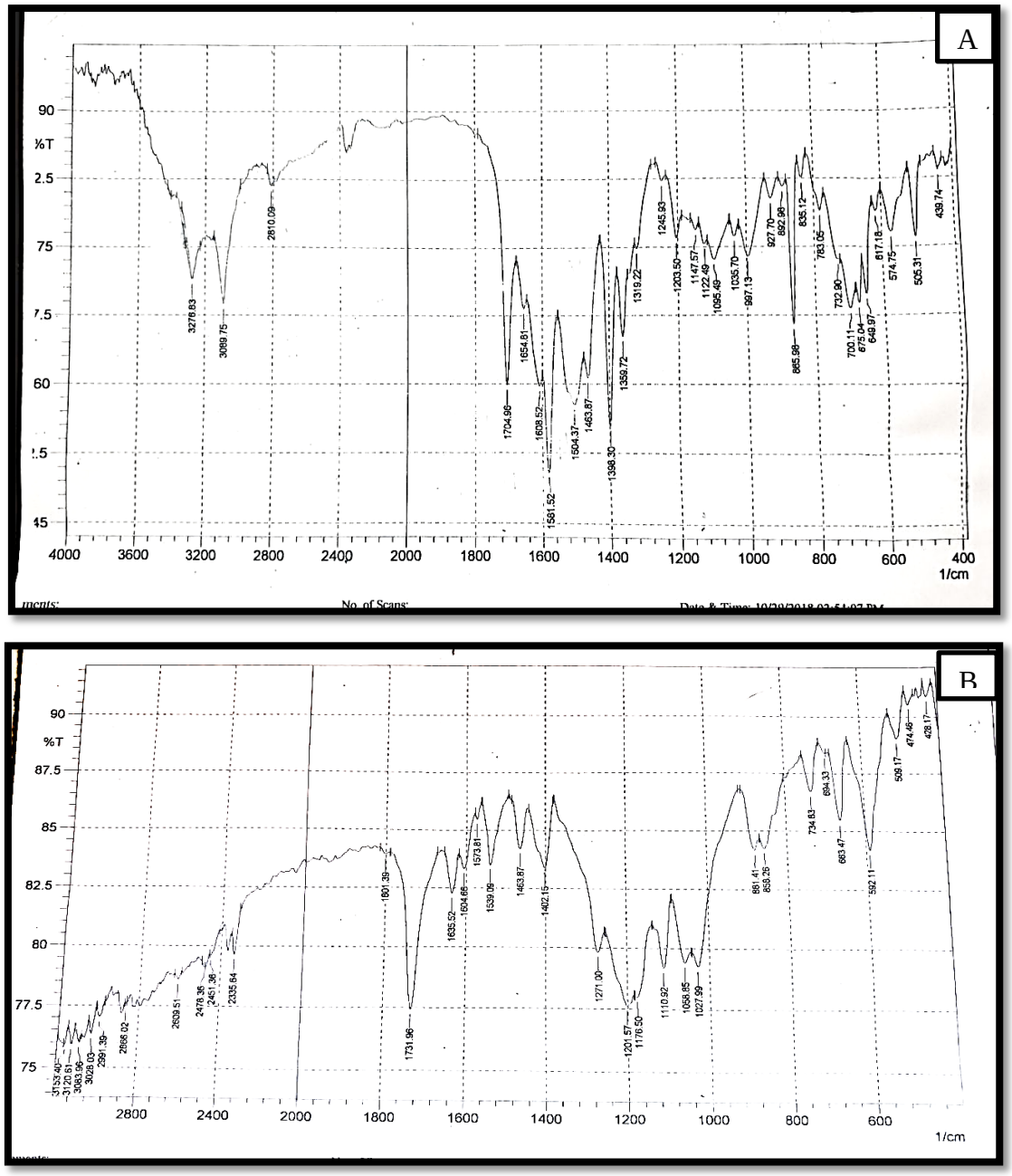

Figure (2): FT-IR for A-the monomer (NOE), B- the polymer (PNOE)

3.3.2. Atomic Force Microscope

The surface topography of the St.St coated with PNOE in the presence and absence of the nanomaterials (graphene and nano-ZnO) was explored through the AFM technique. Figure-3 shows 2D and 3D AFM images of all applied coating films. Through the AFM analysis, the mean grain size, root mean square (RMS), and roughness average (Ra) are the most commonly used parameters to identify the roughness of the surface. These parameters are listed in Table-1. The results show that the roughness of the surface for all coating films was decreased after the modification of PONE with the nanomaterials due to the decrease in the grain size. Hence, the lower roughness of the surface the better barrier effect for the protection of the coating from corrosion [27]

Table 1-Average diameter, root mean square (RMS), and average roughness (Ra) values

Coating	Mean grain size (nm)	RMS(nm)	Ra(nm)
Coated St.St with PONE	93.35	5.25	4.24
Coated St.St with PONE modified with G	92.41	3.02	2.42
Coated St.St with PONE modified with nanoZnO	85.06	2.01	1.58

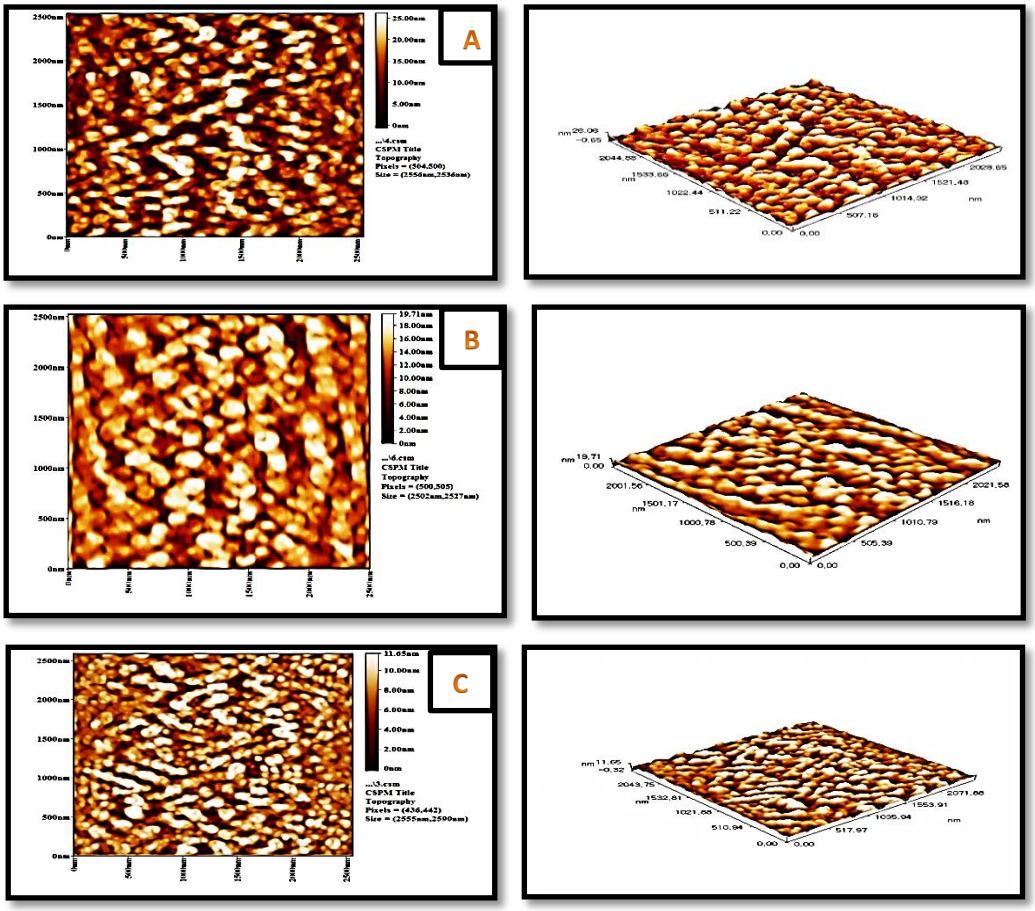

Figure 3-AFM image for (A) PONE, (B) PONE modified with G, (C) PONE modified with nanoZnO.

3.3.3 Scanning Electron Microscope

The surface morphology properties of the PONE films in the presence and absence of the nanomaterial were characterized by SEM. Figures- 4 (A)-(C) shows that PONE has a heterogeneous distribution on the surface of St.St with some pores, while PONE modified with G showed aggregations of spherical grains with different sizes, and PONE modified with nanoZnO showed a homogenous distribution with fibril structure on the surface of St.St [28].

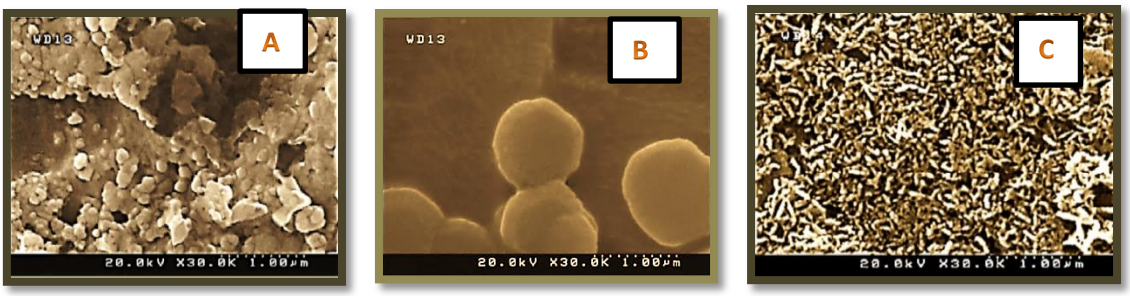

Figure 4-SEM images for (A) polymer (3), (B) PONE modified with G, (C) PONE modified with nano ZnO.

4 - Corrosion Tests

The corrosion of PONE coating film was carried out by using electrochemical polarization. Figure -5 shows typical polarization curves for uncoated and coated 316L St.St with polymer PONE, in the absence and presence of nanomaterial in 0.2M of HCl solution at different temperature (293-323) K. The corrosion potential (E_{corr}) and corrosion current density (i_{corr}) were determined by the extrapolation of the cathodic and anodic Tafel lines to the point of intersection [29] . The cathodic (βc) and anodic (βa) Tafel slopes were determined from the same Figure-5. Table-2 shows the data of corrosion parameter that include the following: corrosion potential E_{corr} (mV), corrosion current density i_{corr} (μA/cm^2), anodic and cathodic Tafel slopes βa and βc (mV/Dec), weight loss WL(g/m^2.d), penetration loss PL(mm/y), polarization resistance Rp (Ω/cm^2), and protection efficiencies (PE%). The value of PE% was calculated by applying the following equation [30]:

$$PE\% = \left[1 - \frac{(\text{i corr}) \text{ coated}}{(io\ corr)\text{uncoated}}\right] * 100 \quad \ldots\ldots (2)$$

where i_{ocorr} and i_{corr} are the density current values for uncoated and coated 316 St.St, respectively.
While the polarization resistance (Rp) was calculated by using the following Stern -Geary equation [31]:

$$Rp = \frac{\beta a * \beta c}{2.303(\beta a + \beta c)\text{icorr}} \quad \ldots (3)$$

Table 2-Corrosion parameters for uncoated and coated 316 St.St with PONE in absence and presence of nanomaterials in 0.2M of HCl at different temperatures

Coating	T(K)	-E_{corr} (mV)	I_{corr} (μA/cm^2)	-βc (mV/sec)	βa (mV/sec)	WL (g/m^2.d)	PL (mm/y)	PE%	Rp (Ω/cm^2)
Uncoated St.St	293	116.7	18.42	188.7	159.8	1.48	$2*10^{-1}$	-	2039..681
	303	126	21.37	199.1	185.8	1.72	$2.32*10^{-1}$	-	1952.858
	313	206.6	24.35	207.7	220.5	1.96	$2.65*10^{-1}$	-	1906.821
	323	271.8	25.89	171.6	258.5	2.08	$2.82*10^{-1}$	-	1729.746
Coated St.St with PONE	293	63.8	4.67	74.4	94.0	$3.76*10^{-1}$	$5.08*10^{-2}$	74.65	3861.427
	303	67.8	5.65	77.0	94.5	$4.55*10^{-1}$	$6.15*10^{-2}$	73.56	3260.739
	313	88.1	8.61	131	128.9	$6.93*10^{-1}$	$9.36*10^{-2}$	64.64	3276.581
	323	122.4	10.39	136.6	170.2	$8.36*10^{-1}$	$1.13*10^{-1}$	59.87	3166.981
Coated St.St with PONE modified with G	293	39.9	1.83	75.6	69.9	$1.48*10^{-1}$	$2*10^{-2}$	90	8617.692
	303	107.8	2.99	87.5	103.5	$2.4*10^{-1}$	$3.25*10^{-2}$	86	6885.729
	313	135.3	3.76	69.6	89.8	$3.02*10^{-1}$	$4.09*10^{-2}$	84.55	4528.094
	323	140.6	6.89	111.2	178.7	$5.54*10^{-1}$	$7.49*10^{-2}$	73.387	4319.843
Coated St.St with PONE modified with nano ZnO	293	79.4	3.09	73.9	68.9	$2.49*10^{-1}$	$3.36*10^{-2}$	83.22	5010.523
	303	142.3	5.25	48.5	50.5	$4.22*10^{-1}$	$5.71*10^{-2}$	75.4	2046.184
	313	195.6	5.93	84.7	95.1	$4.77*10^{-1}$	$6.45*10^{-2}$	75.64	3280.391
	323	245.8	7.97	100.7	111.9	$6.41*10^{-1}$	$8.67*10^{-2}$	69.22	2887.647

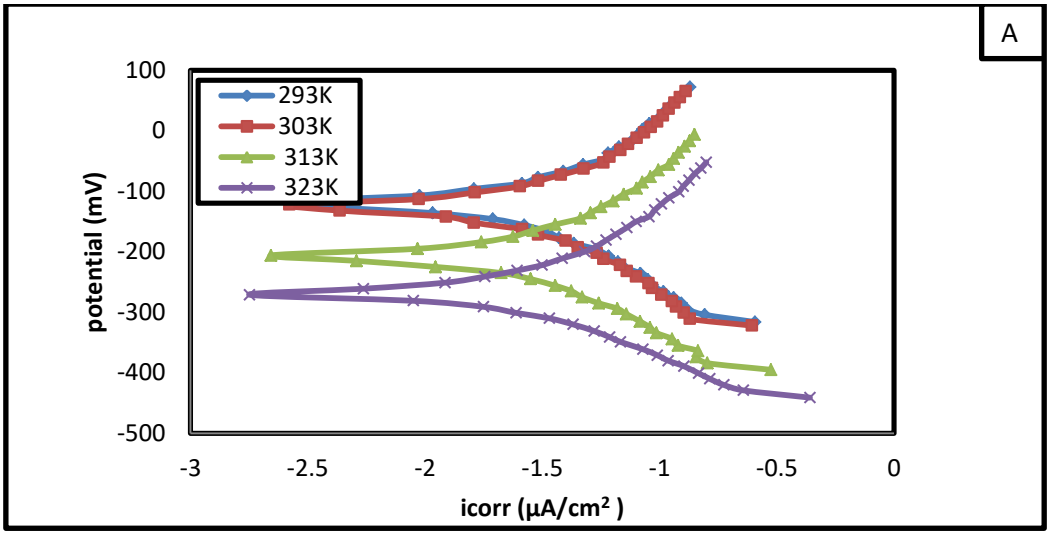

Figure 5-A-Polarization curves for the corrosion of uncoated St.St316L in 0.2M HCl at different temperatures.

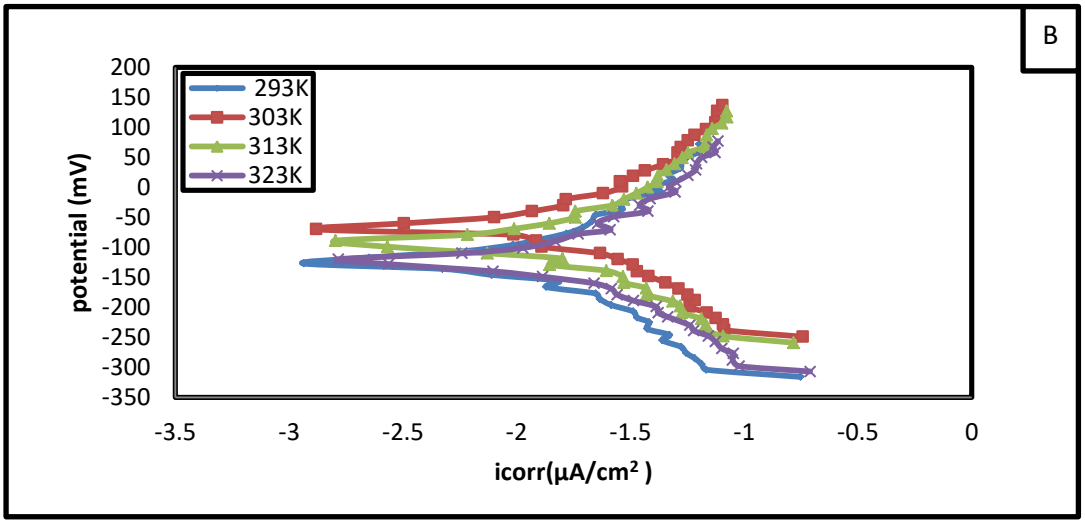

Figure 5-B- polarization curves for the corrosion of coated St.St316L with PONE in 0.2M HCl at different temperatures.

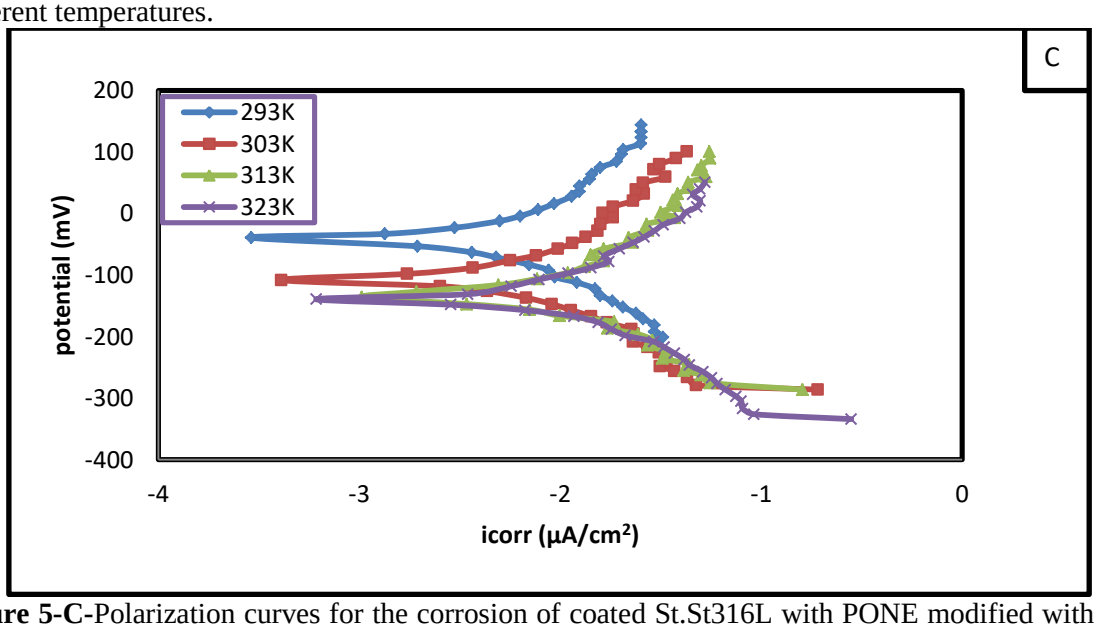

Figure 5-C-Polarization curves for the corrosion of coated St.St316L with PONE modified with G in 0.2M HCl at different temperatures.

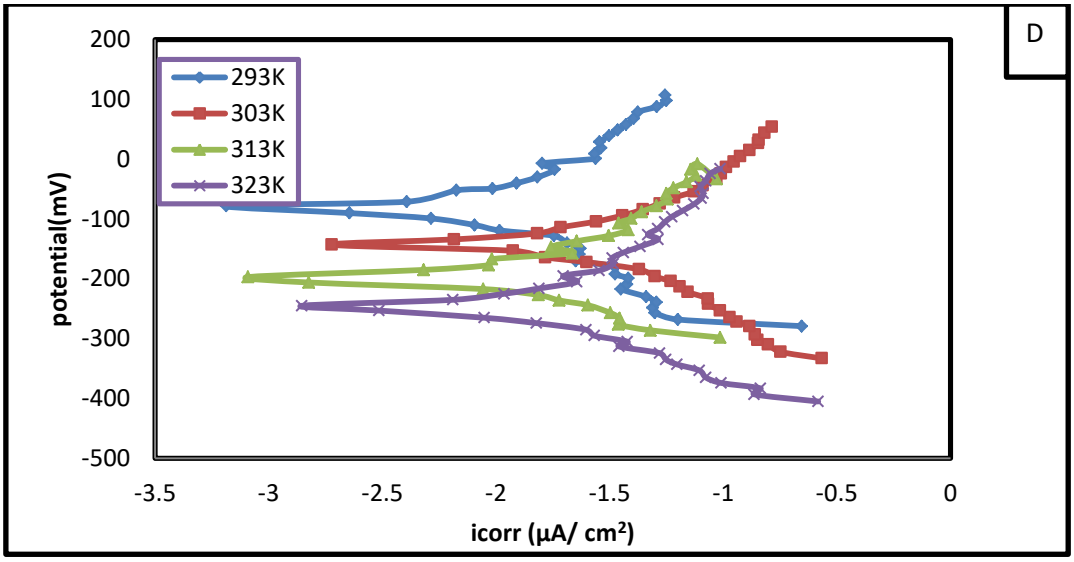

Figure 5-D-Polarization curves for the corrosion of coated St.St316L with PONE modified with nano ZnO in 0.2M HCl at different temperatures.

It is clear from the resulting data that the corrosion potential (E_{corr}) and the corrosion current density (i_{corr}) were increased with the increase in temperature. E_{corr} was shifted to more active values (cathodic) with rising temperatures. The corrosion current density of the coated St.St was significantly decreased compared with that of the uncoated St.St, , after adding the nanomaterial. Also, it was observed from the Tafel plots that the E_{corr} for the coated S.S was shifted into a higher position (noble direction) as compared to that for the blank S.S. This indicates that the corrosion protection acts as an anodic protection [32, 33]. Also, the Rp values showed a greater increase in the coated than in the uncoated St.St, especially after adding the nanomaterials.

5- Kinetics and thermodynamics of the coated St.St316L

The effects of temperature on the corrosion rate of uncoated and coated St.St316L in 0.2M of HCl solution were studied for the temperature range of 293-323 K by using Arrhenius equation [34].

$$i_{corr} = A\ exp\left(\frac{-Ea}{RT}\right) \quad \ldots\ldots (4)$$

Equation (3.4) was converted into the logarithmic form, as follows:

$$\text{Log i corr} = LogA - \frac{Ea}{2.303RT} \quad \ldots. \ (5)$$

While the transition state equation was expressed as follows:[35]

$$Log\frac{i\ corr}{T} = Log\left[\frac{R}{Nh} + \frac{\Delta S*}{2.303R}\right] - \frac{\Delta H*}{2.303RT} \quad \ldots\ (6)$$

where i_{corr} : corrosion current density, T : absolute temperature (K), Ea: activation energy, A: pre-exponential factor , R: gas constant (8.315 J/K.mol^{-1}), N: the Avogadro's number (6.022 x 10^{23} mol^{-1}), h: Planck's constant (6.626176x10^{-34} J.S), ΔS*: the entropy of activation, and ΔH*: the enthalpy of activation.

Figure-6 shows Arrhenius plots for the corrosion of coated and uncoated St.St in 0.2 M of HCl solution. Figure-7 shows the plots of log (i_{corr} /T) versus 1/T. The values of the enthalpy change of activation (ΔH*) and the entropy change of activation (ΔS*) were obtained from the slopes and intercepts, respectively. The activation Gibbs free energy (ΔG*) was calculated by using the following equation [36]:

$$\Delta G* = \Delta H* - T\Delta S* \quad \ldots\ldots \quad (7)$$

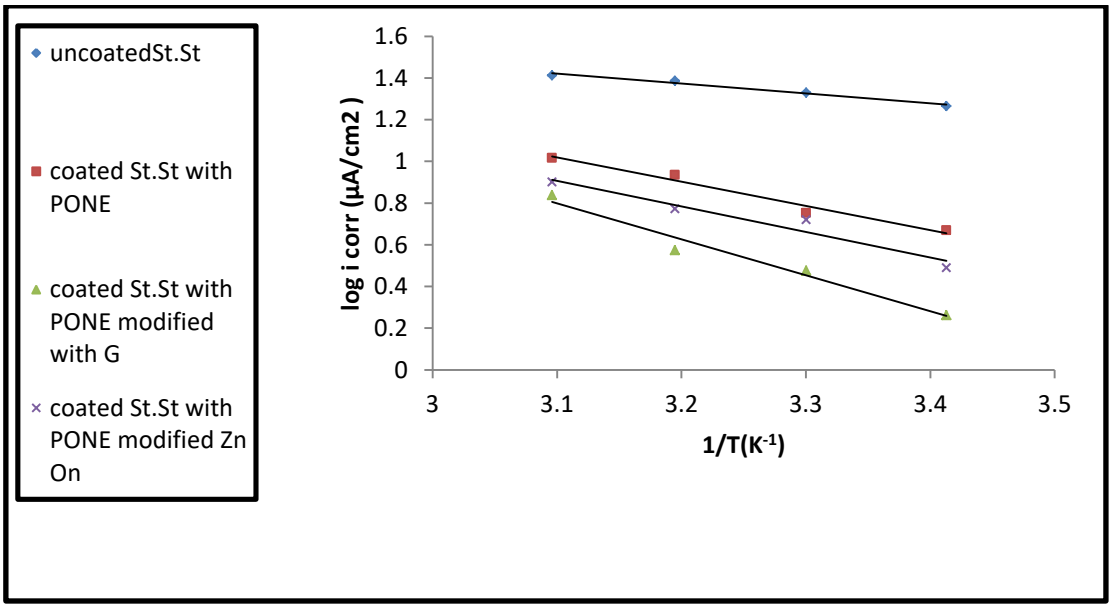

Figure 6-Plot of log i_{corr} vs. 1/T for uncoated and coated St.St with PONE in the absence and presence of nanomaterials in 0.2M HCl.

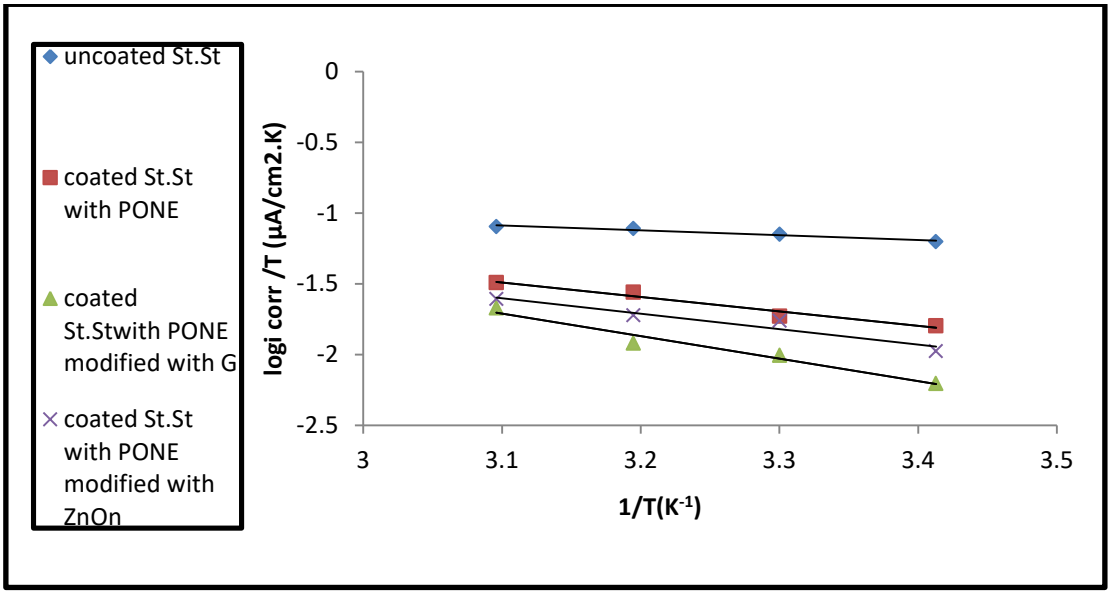

Figure 7-Plot of log i_{corr}/T vs. 1/T for uncoated and coated St.St with PONE in the absence and presence of nanomaterials in 0.2M HCl.

Table 3- Transition state's thermodynamic parameters at different temperatures for the corrosion of uncoated and coated St.St with PONE in the absence and presence of nanomaterials in 0.2M HCl solution

Coating	T(K)	ΔG* (kJ/mol)	ΔH* (kJ/mol)	-ΔS* (J/mol.K)	R^2	Ea (kJ/mol)	A (Molecule. $cm^{-2}.S^{-1}$)	R^2
Uncoated St.St	293	64.593	6.546	198.112	0.958	9.103	$4.721*10^{26}$	0.979
	303	66.574						
	313	68.555						
	323	70.536						

coated St.St with PONE	293	68.049	19.624	165.276	0.966	22.180	$2.449*10^{28}$	0.973
	303	69.703						
	313	71.355						
	323	73.008						
coated St.St with PONE modified with G	293	70.277	30.471	135.858	0.965	33.027	$8.421*10^{29}$	0.969
	303	71.636						
	313	72.995						
	323	74.353						
coated St.St with PONE modified with ZnOn	293	68.794	20.879	163.528	0.929	23.426	$3.022*10^{28}$	0.944
	303	70.429						
	313	72.064						
	323	73.699						

All the calculated values of kinetics and thermodynamic parameters are listed in Table-3. The results show that the activation energies in the presence of PNOE film were increased, indicating a higher protection efficiency as a result of coating. The values of activation energies were increased with adding different nanomaterials, which indicates an increase in the energy barrier for the corrosion reaction. The positive sign of the activation enthalpies (ΔH*) for coated and uncoated St.St indicates the endothermic nature of the transition state reaction of St.St. The values of ΔS * for the coated and uncoated St.St are negative, implying that the activation complex in the rate- determining step represents an association rather than a dissociation step. This indicates a decrease in the disordering which takes place during the transition from the reactant to the activated complex [37- 38]. The positive values of ΔG* listed in Table-3 show nearly small change with the rise in temperature and indicate the non-spontaneous nature of the transition state for the uncoated and coated St.St.

5- Antibacterial activity

Polymeric coatings have a diverse use in most of the pharmaceutical and biomedical applications. The results of biological activity of the polymer, with and without nanomaterial, are listed in Table- 4. A good inhibition activity was observed for PONE, compared with Amoxicillin, against Gram-negative bacteria (*Escherichia coli*) and Gram-positive bacteria (*Staphylococcus aureus*). Also, the ability of PONE to kill bacteria was increased after the modification with nano-materials, especially with graphene [39].

Table 4-Biological activity of the tested polymer and polymer nanomaterial

System	Gram positive (*S. aureus*)	Gram negative (*E. coli*)
PONE	12	13
PONE+G	14	16
PONE+nanoZnO	13	18
Amoxicillin	30	30

Solvent DMSO: [C]: 800 µg/ ml

Conclusions

The electro polymerization of NOE on St.St acted as a good anti-corrosion coating in 0.2M HCl. The PE% and polarization resistance (Rp values of the coating polymer were decreased with

temperature increase. The PE% value was also increased after adding the nanomaterial, especially graphene . The corrosion current density was increased with rising temperature, while the corrosion potential was decreased with increasing temperature. The corrosion potential was moved to the noble direction , where it was acting as an anodic protection. SEM and FAM analyses showed the protection of St.St due to the formation of a protective coating on its surface. Also, the biological activity of the polymer film was modified, with the nanomaterial having a moderate activity against Gram-positive and negative bacteria.

References

1. Shih, C.-C., et al., **2004** . Effect of surface oxide properties on corrosion resistance of 316L stainless steel for biomedical applications. *Corrosion Science*, **46**(2): 427-441.
2. Ruhi, G., O. Modi, and I. Singh.**2009**. Pitting of AISI 304L stainless steel coated with nano structured sol–gel alumina coatings in chloride containing acidic environments. *Corrosion Science*, **51**(12): 3057-3063.
3. Nessrain A.Hussain, Nadia Abraheem Fakry and Huda Ali Alpana. **2013**. Composite Resin Coating for The protection of Surfaces and Metals . *Iraqi Journal of Science*, **54**(1): 110-114.
4. Manickavasagam, R., et al. **2002**. Poly (styrene sulphonic acid)-doped polyaniline as an inhibitor for the corrosion of mild steel in hydrochloric acid. *Anti-Corrosion Methods and Materials* .
5. Sadki, S., et al. **2000**. The mechanisms of pyrrole electropolymerization. *Chemical Society Reviews*, **29**(5): 283-293.
6. Wang, L.-X., X.-G. Li, and Y.-L. Yang. **2001.** Preparation, properties and applications of polypyrroles. *Reactive and Functional Polymers*, **47**(2): 125-139.
7. Malinauskas, A. **2001**. Chemical deposition of conducting polymers. *polymer*, **42**(9): 3957-3972.
8. Wencheng, S. and Iroh, J.O. **1998** . Effects of electrochemical process parameters on the synthesis and properties of polypyrrole coatings on steel. *Synthetic metals*, . **95**(3): 159-167.
9. Meerholz, K. and Heinze, J. **1993**. Influence of chain length and defects on the electrical conductivity of conducting polymers. *Synthetic metals*, **57**(2-3): 5040-5045.
10. Sayyah, S. and Azooz**, R. 2016**. Electrosynthesis and characterization of adherent poly (2-aminobenzothiazole) on Pt-electrode from acidic solution. *Arabian Journal of Chemistry*, **9**: S576-S586.
11. Rosa, R.M., et al. **2005**. Conducting Polymer-Based Chemiresistive Sensor for Organic Vapours. in Macromolecular symposia. *Wiley Online Library*.
12. Arulepp, M., et al.**2004**. Influence of the solvent properties on the characteristics of a double layer capacitor. *Journal of Power Sources*, **133**(2): 320-328.
13. Song, H.K. and Palmore, G.T.R. **2006**. Redox-active polypyrrole: toward polymer-based batteries. *Advanced Materials*, **18**(13): 1764-1768.
14. Saxena, V. and Malhotra. **B. 2003**. Prospects of conducting polymers in molecular electronics. *Current Applied Physics*, **3**(2-3): 293-305.
15. Mansouri, J. and Burford, R. **1994**. Novel membranes from conducting polymers. *Journal of membrane science*, **87**(1-2): 23-34.
16. Qin, Q., J. Tao, and Yang, Y. **2010**. Preparation and characterization of polyaniline film on stainless steel by electrochemical polymerization as a counter electrode of DSSC. *Synthetic Metals*, **160**(11-12): 1167-1172.
17. Kenawy, E.R**. 2001**. Biologically active polymers. IV. Synthesis and antimicrobial activity of polymers containing 8-hydroxyquinoline moiety. *Journal of Applied Polymer Science*, **82**(6): 1364-1374.
18. Kenawy, E.-R., S. Worley, and Broughton, R. **2007**. The chemistry and applications of antimicrobial polymers: *a state-of-the-art review*. *Biomacromolecules*, **8**(5): 1359-1384.
19. Saleh, K.A. and Ali**,** M.I. **2020**. Electro polymerization for (N-Terminal tetrahydrophthalamic acid) for Anti-corrosion and Biological Activity Applications. *Iraqi Journal of Science* : 1-12.
20. William, S., J. Hummers, and Offeman, R.E. **1958**. Preparation of graphitic oxide. *J. Am. Chem. Soc*, **80**(6): 1339-1339.
21. Ariyanayagam, D.K . **2012**. Advanced electrode materials for electrochemical supercapacitors.

22. Léonard-Stibbe, E., et al. **1994**.The cationic polymerization of N-vinyl-2-pyrrolidone initiated electrochemically by anodic polarization on a Pt surface. *Journal of Polymer Science Part A: Polymer Chemistry*, **32**(8): 1551-1555.
23. Mahla, D.K., et al**. 2013**. Morphology and cyclic voltammetry analysis of in situ polymerized polyaniline/graphene composites. *Journal of Electrochemical Science and Engineering*, **3**(4): 157-166.
24. Silverstein, R.M. and G.C. Bassler. **1962**. Spectrometric identification of organic compounds. *Journal of Chemical Education*, **39**(11): 546.
25. Shriner, R.L., R. Fuson, and D.Y. Curtin . **1948**. Thesystematic identification of organic compounds. *John Wiley and Sons, New York*, : 202-207.
26. Koj, N. **1962**. Infrared abstraction spectroscopy. *Nankodo Company Limited, Tokyo*
27. Karthikeyan, P., M Malathy, and R. Rajavel**.2017**. Poly (ophenylenediaminecoaniline)/ZnO coated on passivated low nickel stainless steel. *Journal of Science: Advanced Materials and Devices*, **2**(1): 86-92.
28. Alves, K.G., et al .**2012.** Characterization of ZnO/polyaniline nanocomposites prepared by using surfactant solutions as polymerization media. *Journal of Applied Polymer Science*, **125**(S1): 141-147.
29. Heitz, E. and Schwenk, W. **1976**. Theoretical Basis for the Determination of Corrosion Rates from Polarisation Resistance: Report prepared for the European Federation of Corrosion Working Party on 'Physicochemical Testing Methods of Corrosion—Fundamentals and Application*'. British Corrosion Journal*, **11**(2): 74-77.
30. Bentiss, F., M. Lebrini, and Lagrenée, M. **2005**. Thermodynamic characterization of metal dissolution and inhibitor adsorption processes in mild steel/2, 5-bis (n-thienyl)-1, 3, 4-thiadiazoles/hydrochloric acid system. *Corrosion Science*, **47**(12): 2915-2931.
31. Lorenzetti, M., et al. **2014**. Improvement to the corrosion resistance of Ti-based implants using hydrothermally synthesized nanostructured anatase coatings. *Materials*, **7**(1): 180-194.
32. Dariva, C.G. and Galio, A.F. **2014**. Corrosion Inhibitors – Principles, Mechanisms and Applications, in Developments in Corrosion Protection.
33. Kassou, O., et al.**2015**. Comparative study of low carbon steel corrosion inhibition in 200 ppm NaCl by amino acid compounds. *J. Mater. Environ. Sci*, **6**: 1147-1155.
34. Fontana, M.G., M.-H. **1987**. *Corrosion Engineering*. New York (3) : 3rd ed. .
35. Joseph, B., et al. **2010**. Imidazolidine-2-thione as corrosion inhibitor for mild steel in hydrochloric acid.
36. Mobin, M., S. Zehra, and Parveen, M. **2016.** L-Cysteine as corrosion inhibitor for mild steel in 1 M HCl and synergistic effect of anionic, cationic and non-ionic surfactants. *Journal of Molecular Liquids*, **216**: 598-607.
37. Abdallah, M. **2002**. Rhodanine azosulpha drugs as corrosion inhibitors for corrosion of 304 stainless steel in hydrochloric acid solution. *Corrosion Science*, **44**(4): 717-728.
38. Noor, E.A. and A.H. Al-Moubaraki. **2008**.Thermodynamic study of metal corrosion and inhibitor adsorption processes in mild steel/1-methyl-4 [4′(-X)-styryl pyridinium iodides/hydrochloric acid systems. *Materials Chemistry and Physics*, **110**(1): 145-154.
39. Roselli, M., et al. **2003**. Zinc oxide protects cultured enterocytes from the damage induced by Escherichia coli. *The Journal of nutrition*, **133**(12): 4077-4082.